Future prospects for cryoEM

EMBO practical course
Image processing for cryoEM

11th September 2019

Richard Henderson

From Baker & Henderson (2001) Int.Tab.Cryst.Vol.F, on-line (2006), revised (2011)

What is electron cryomicroscopy? - CryoEM comes in several flavours

70S ribosome 11 Å | hepatitis B cores 7 Å | decorated actin 30 Å | LHC II 3.4 Å

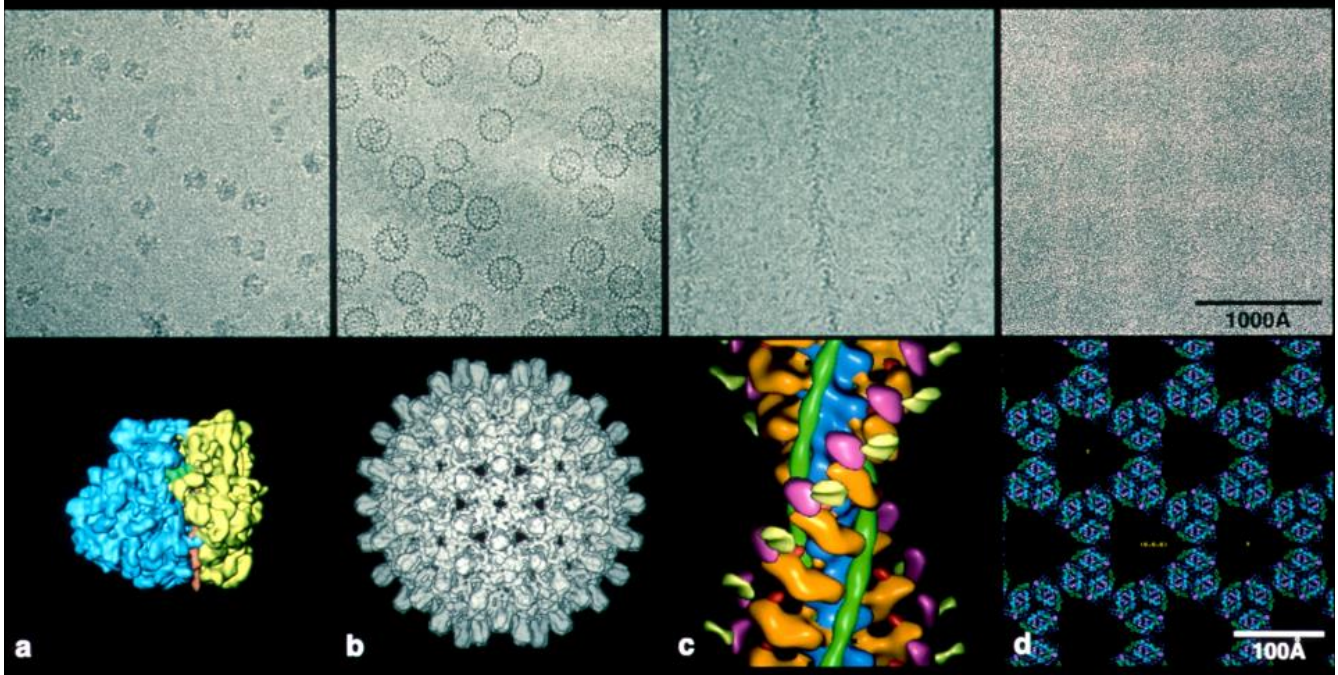

Gabashvili (2000) | Boettcher (1997) | Milligan (~1995) | Kuhlbrandt (1994)

From Dubochet et al, QRB (1988)

Alasdair McDowall & Marc Adrian, liquid ethane and blotting unsupported thin film

Cryo-electron microscopy of vitrified specimens 199

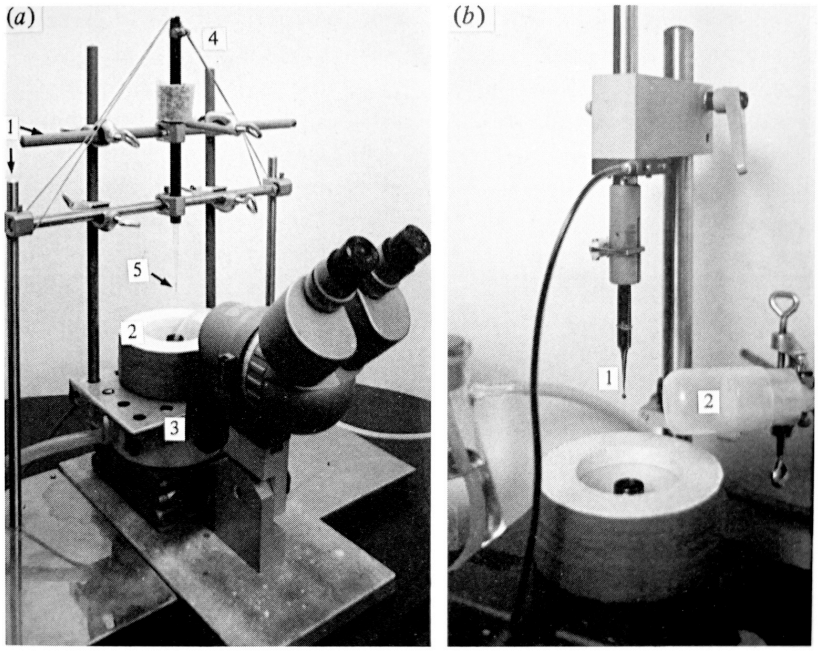

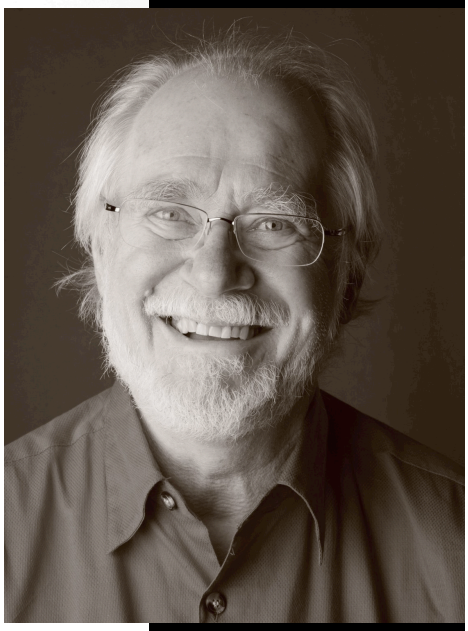

Fig. 43. Plunger for freezing. (*a*) Simple apparatus equipped here for freezing bulk specimens. (1) Retort stand clamps; (2) liquid nitrogen and ethane dewars; (3) water-driven magnet; (4) plunger with elastic band propulsion; (5) specimen support. (*b*) A more elegant freezing apparatus equipped for preparing thin vitrified layers of suspensions. (1) Tweezer holding the specimen support grid; (2) humidified air outlet.

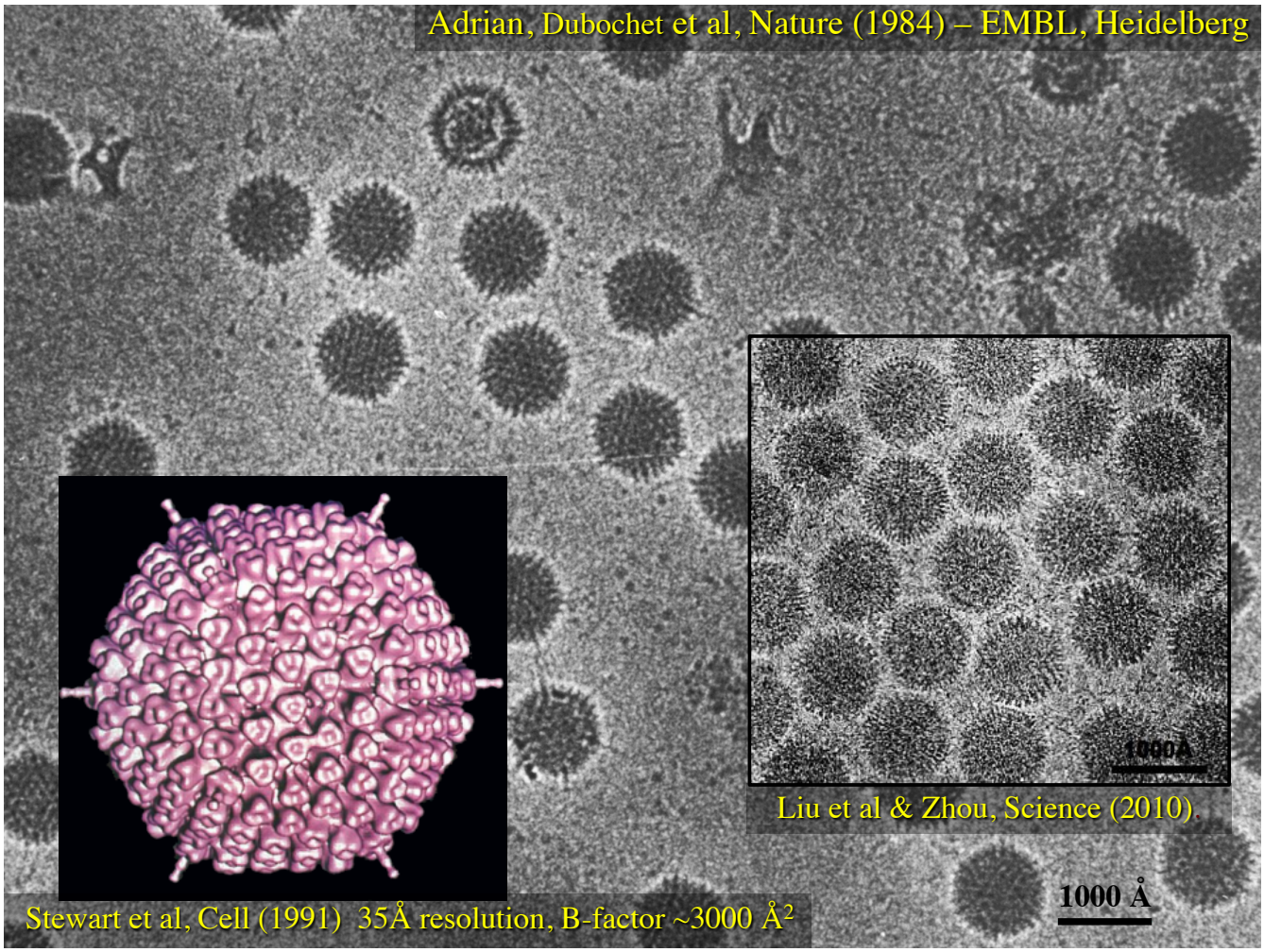

Adrian, Dubochet et al, Nature (1984) – EMBL, Heidelberg

Liu et al & Zhou, Science (2010).

Stewart et al, Cell (1991) 35Å resolution, B-factor ~3000 Å^2

Atomic structure of human adenovirus by Cryo-EM

Liu et al & Zhou, Science (2010), JMB (2011).

3.6Å resolution, B=300Å^2
300keV on film

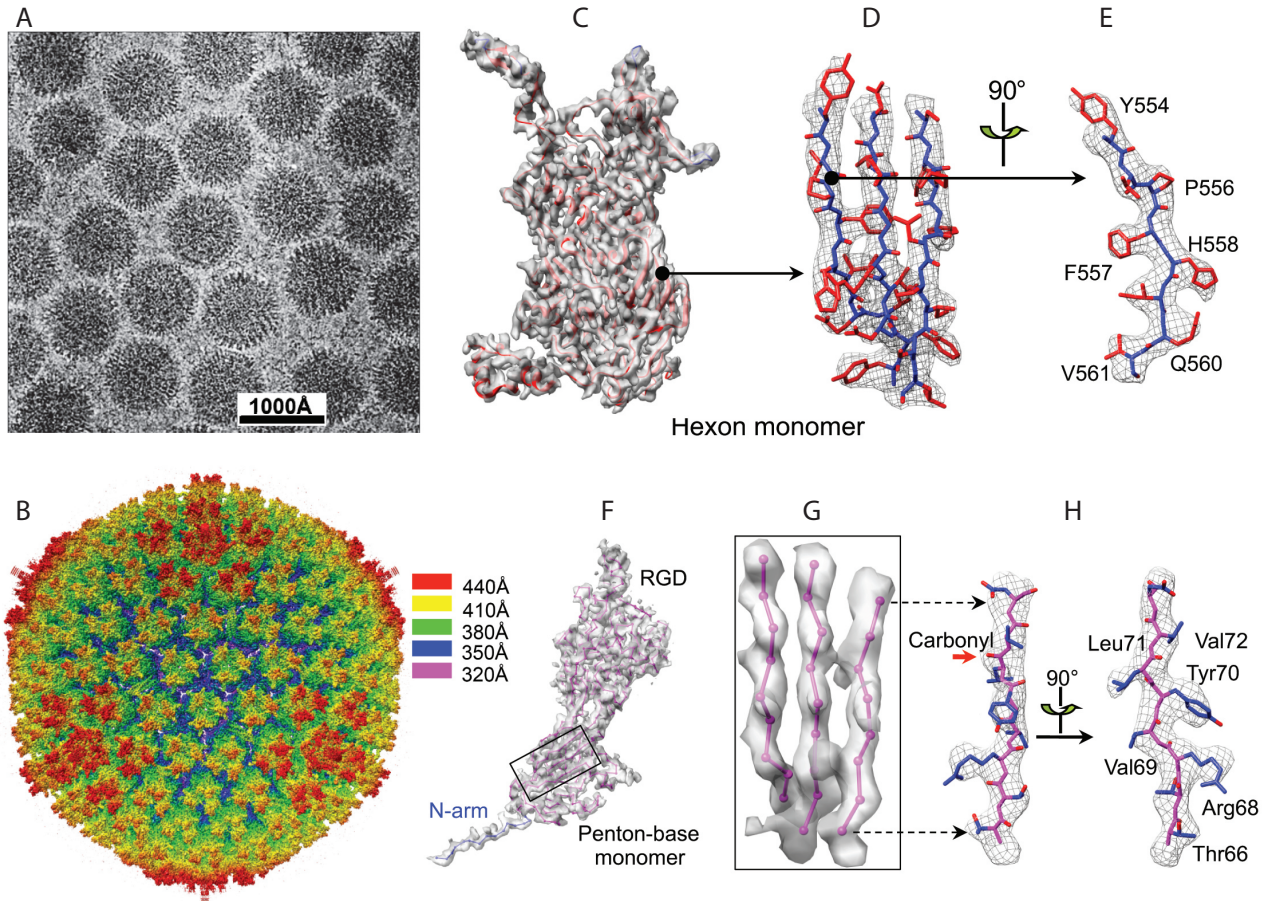

Comparison of 300keV DQE of direct electron detectors versus film

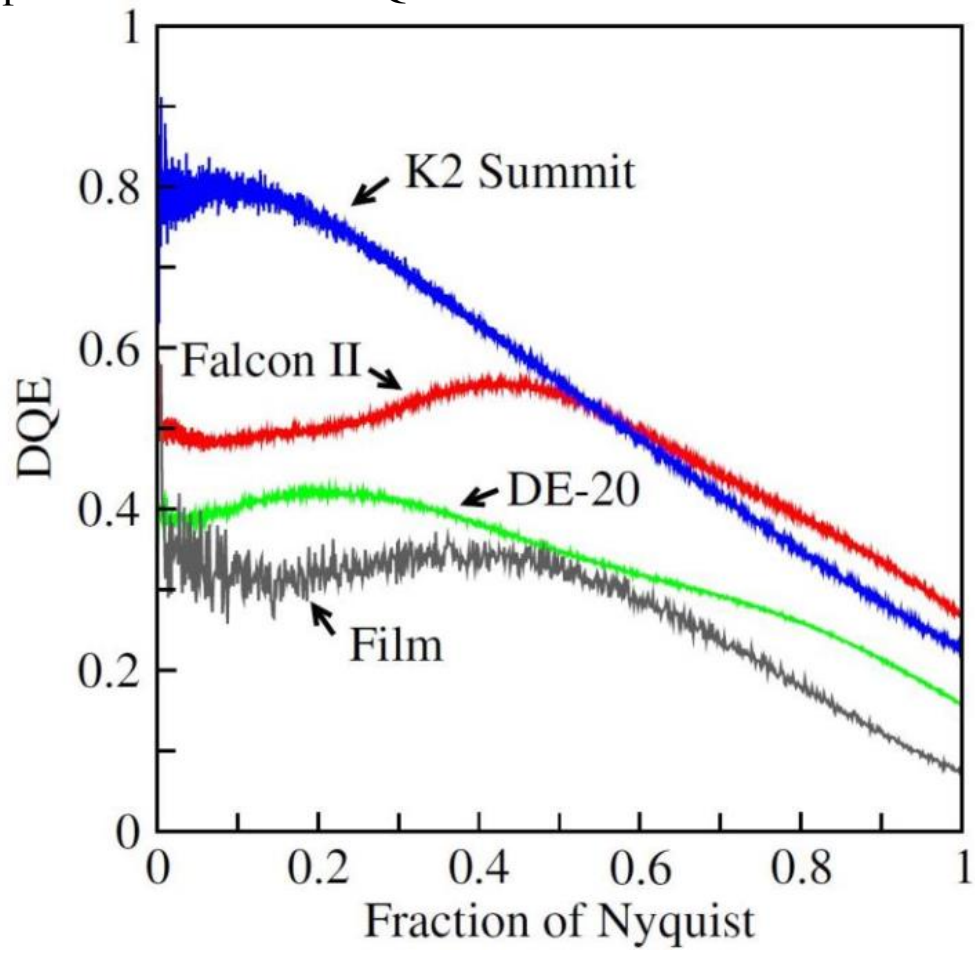

3.1 Å mitochondrial ribosome map 300keV, Falcon, Amunts et al, Science **343**, 1485-1489 (2014)
(groups of Scheres & Ramakrishnan)

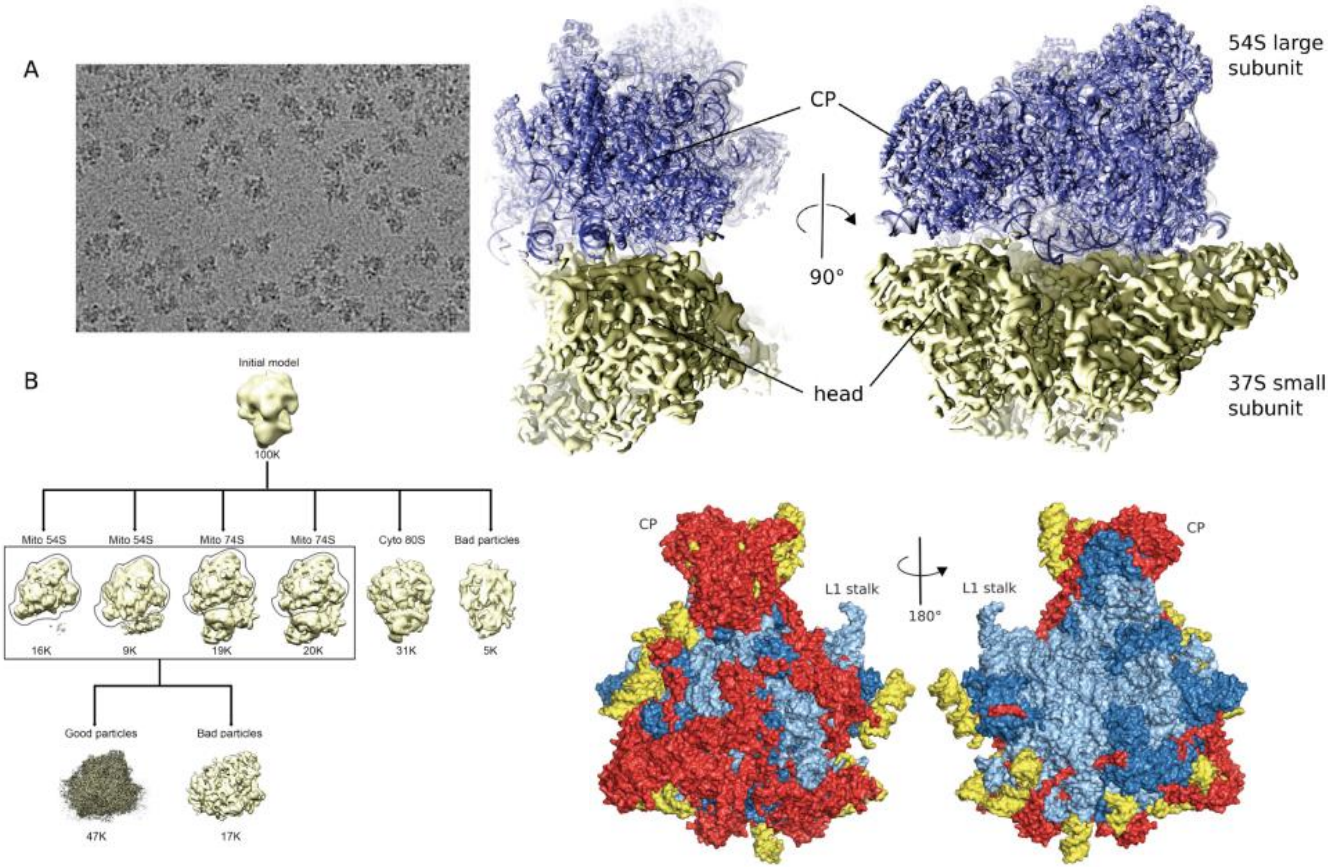

3.1 Å mitochondrial ribosome map 300keV, Falcon, Amunts et al, Science **343**, 1485-1489 (2014)
(groups of Scheres & Ramakrishnan)

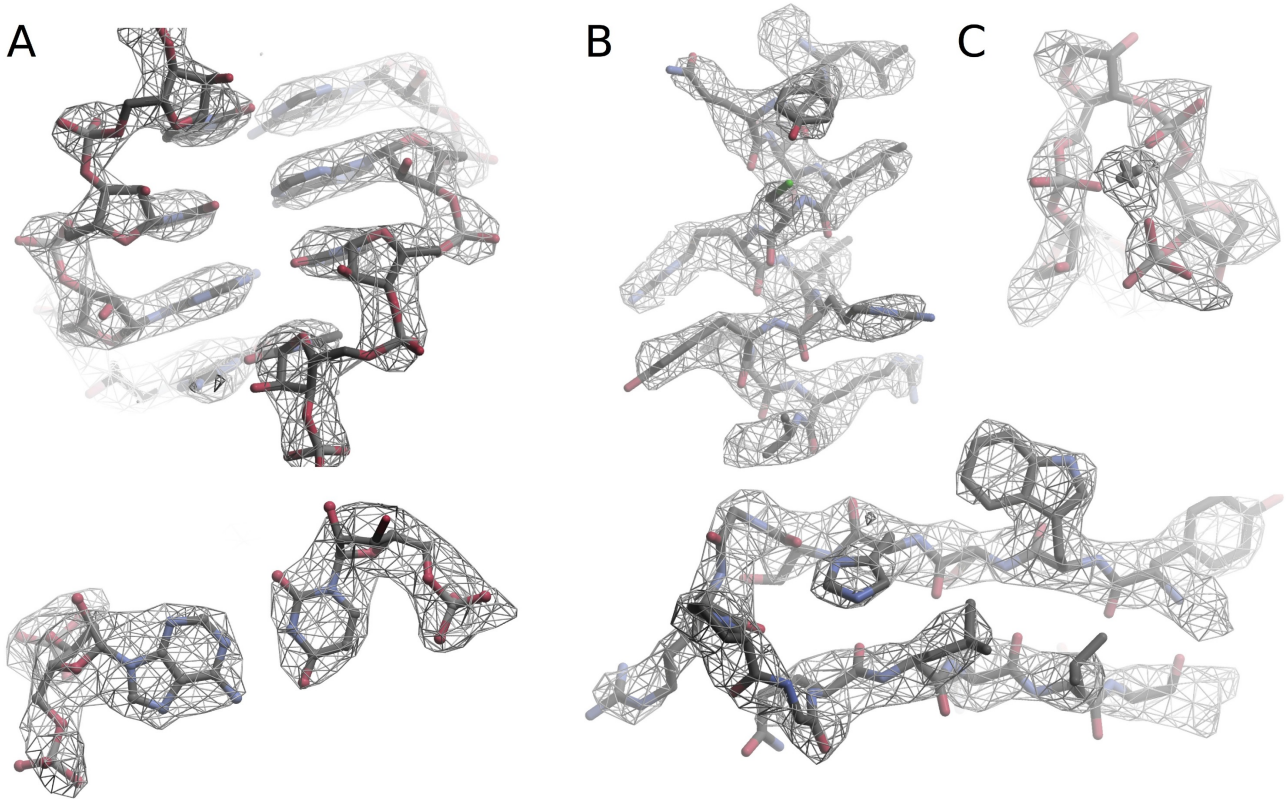

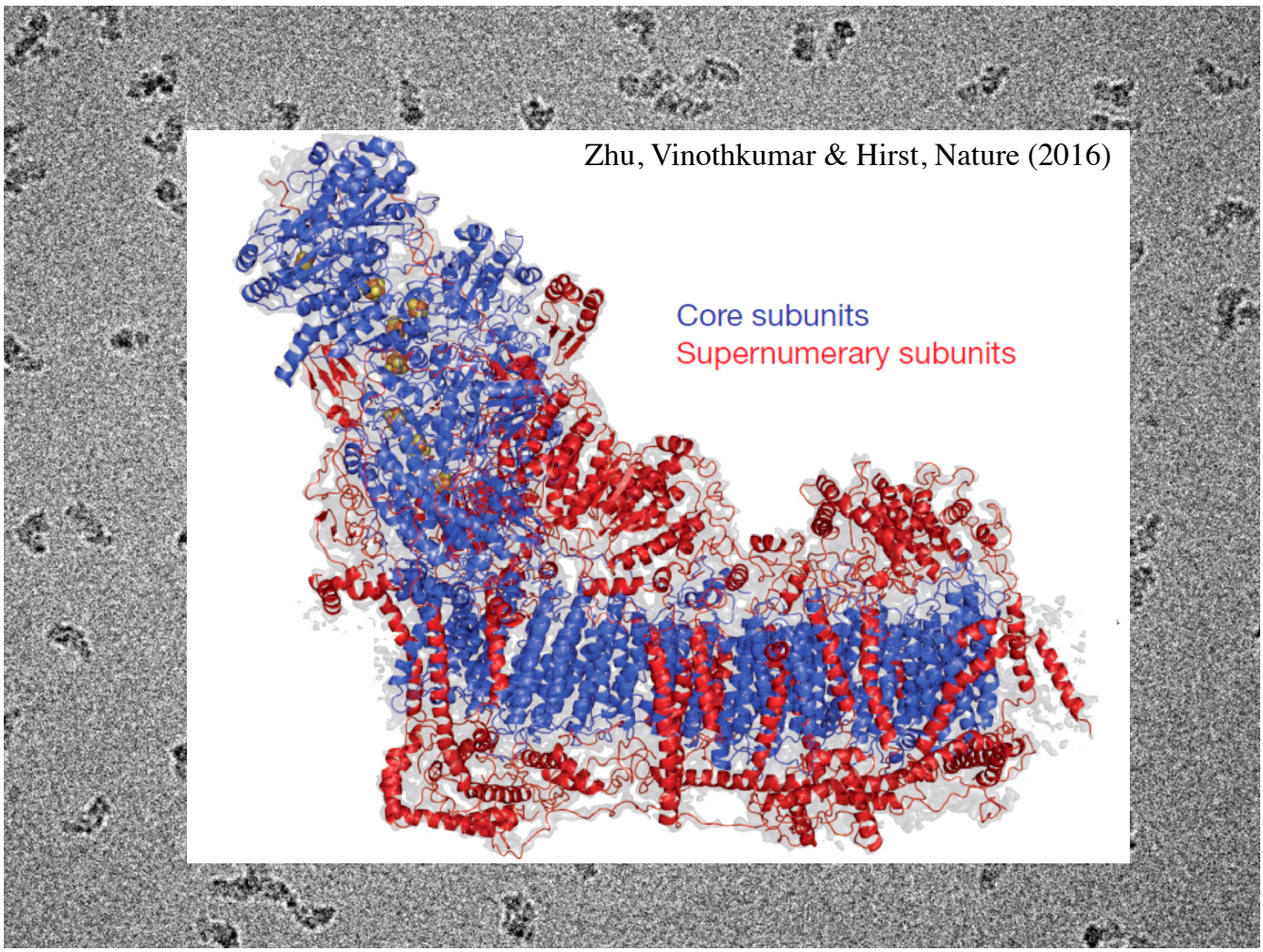

Statistics from Worldwide Protein Data Bank (wwPDB)

Total coordinates deposited 150,145

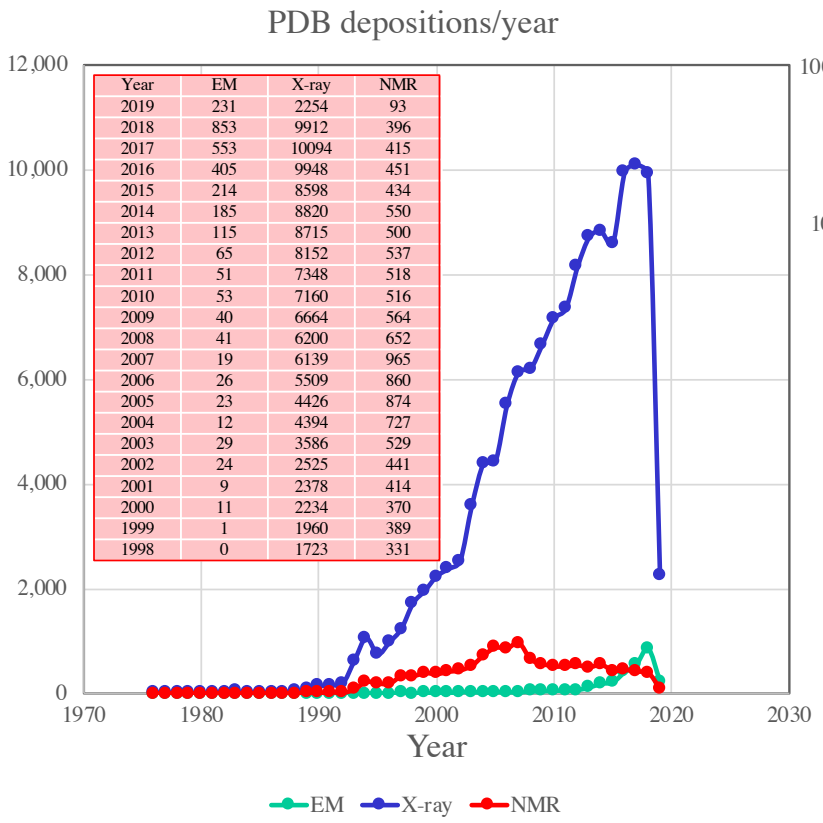

Year	EM	X-ray	NMR
2019	231	2254	93
2018	853	9912	396
2017	553	10094	415
2016	405	9948	451
2015	214	8598	434
2014	185	8820	550
2013	115	8715	500
2012	65	8152	537
2011	51	7348	518
2010	53	7160	516
2009	40	6664	564
2008	41	6200	652
2007	19	6139	965
2006	26	5509	860
2005	23	4426	874
2004	12	4394	727
2003	29	3586	529
2002	24	2525	441
2001	9	2378	414
2000	11	2234	370
1999	1	1960	389
1998	0	1723	331

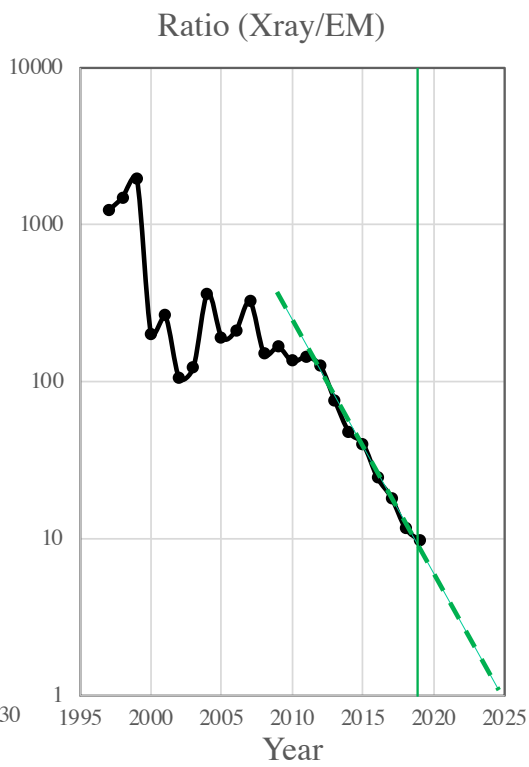

Rosenthal (2003) JMB **333**, 225-36

Theory – single particles in ice

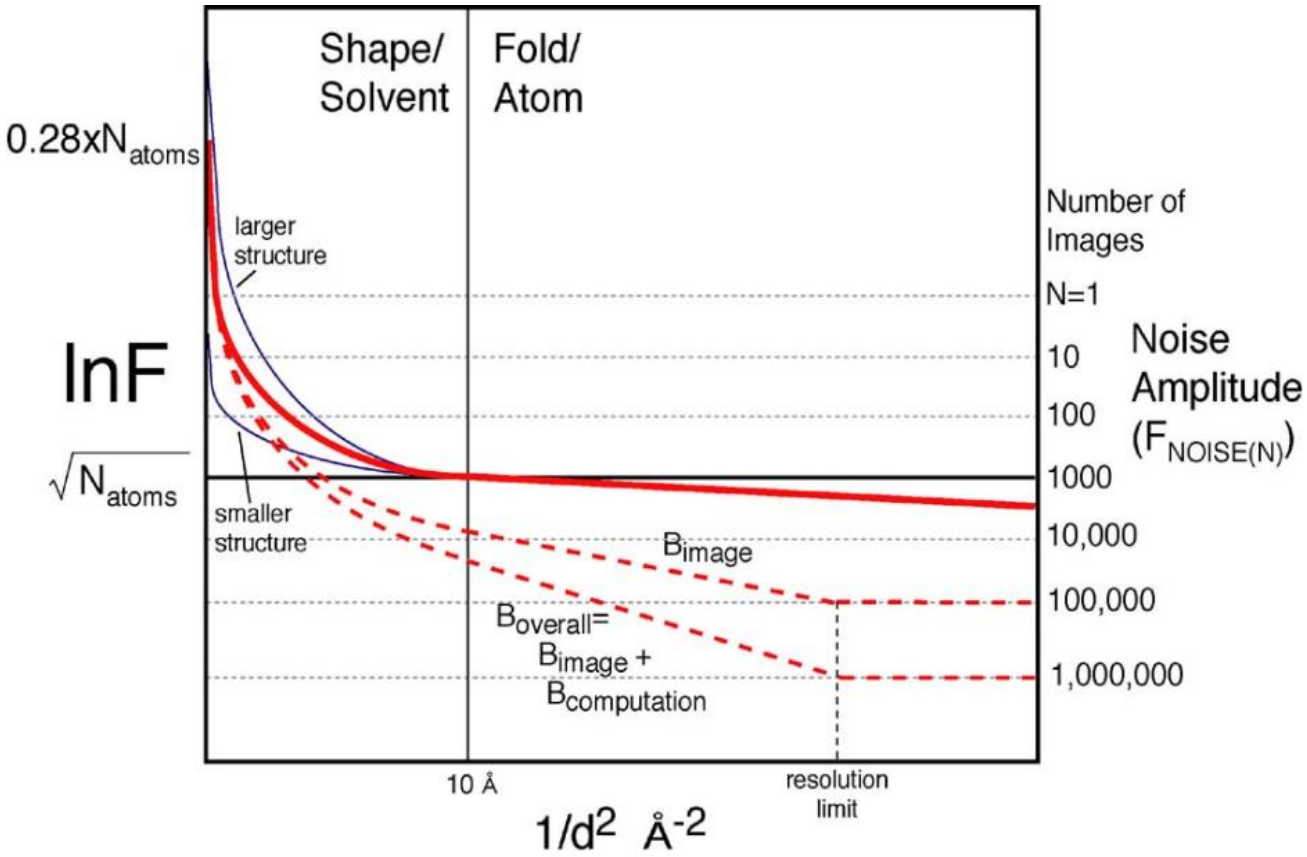

Rosenthal (2003) JMB **333**, 225-36
Fernandez (2008) JSB **164**, 170-5

Experimental data

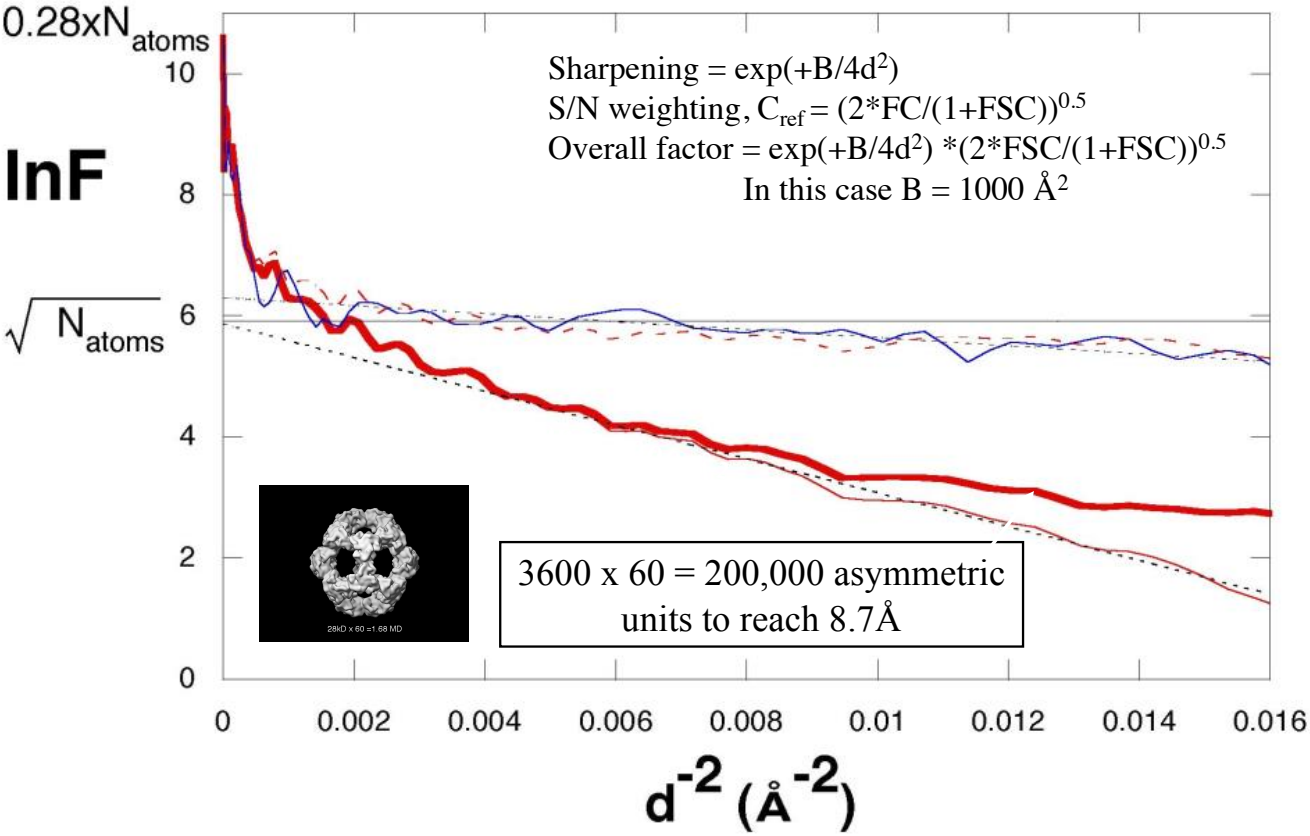

Rosenthal (2003) JMB **333**, 225-36

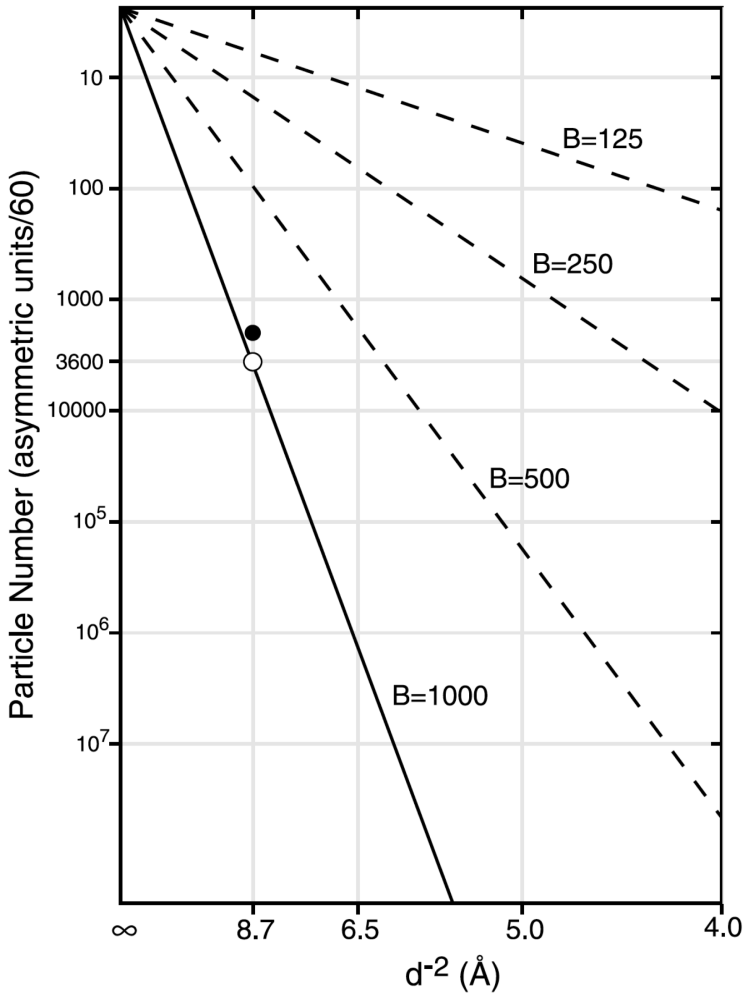

Influence of B-factor on number of particles required to reach different resolutions.

Resolution vs. number of particles

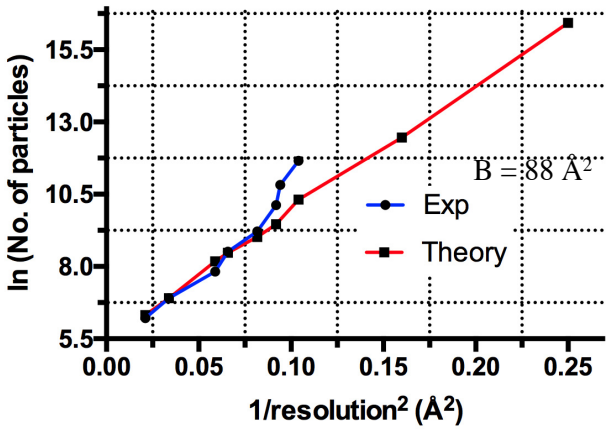

Plot of number of particles versus resolution should be linear if a single B-factor describes the average structure factor.

These three examples needed ~5000 asymmetric units to reach 4Å resolution, ~1500 to reach 6Å, 800 to 10Å.

Reducing B-factor is key to high resolution without unrealistic numbers of particles

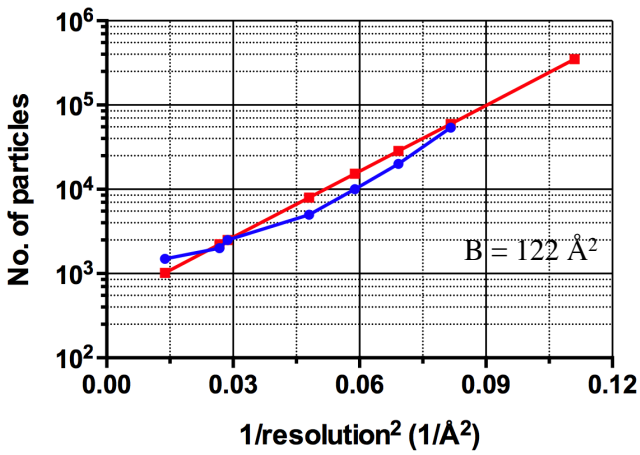

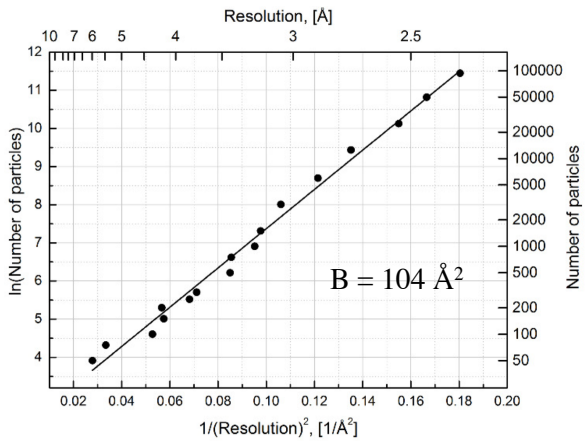

Danev et al, eLife 2017

Information content in movie frames from 4 different datasets

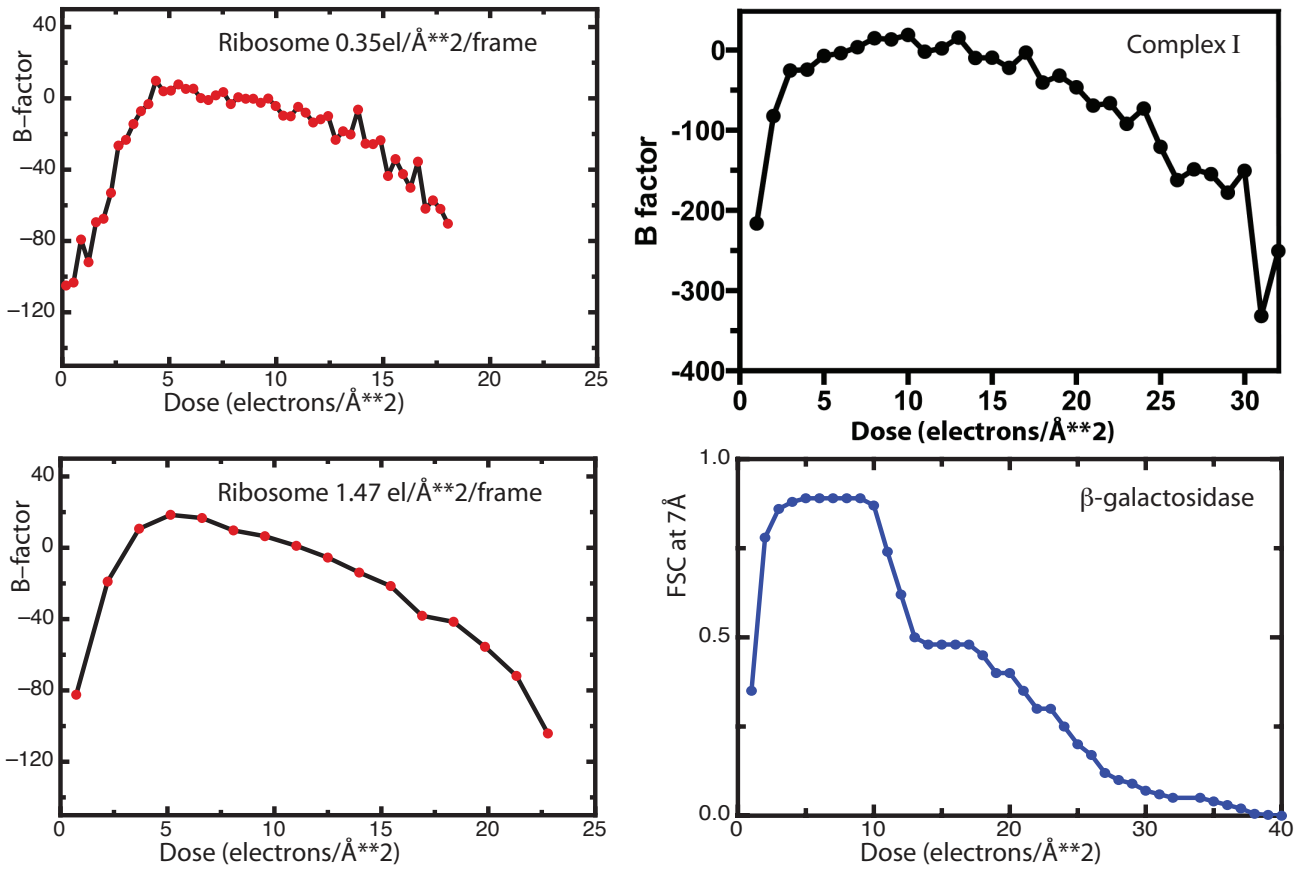

Outstanding issues to be considered

- Charge build up due to loss of secondary electrons (Berriman effect)
- Microscopic charge fluctuations (bees swarm effect)
- Gradual build up of disorder (increased B-factor with increased dose) - radiation damage

- Physical (pseudo-Brownian) motion of water molecules due to radiation damage to water
- Beam-induced motion (a) due to relaxation of stresses created during plunge-freezing
- Beam-induced motion (b) due to bond breakage and release of volatile fragments

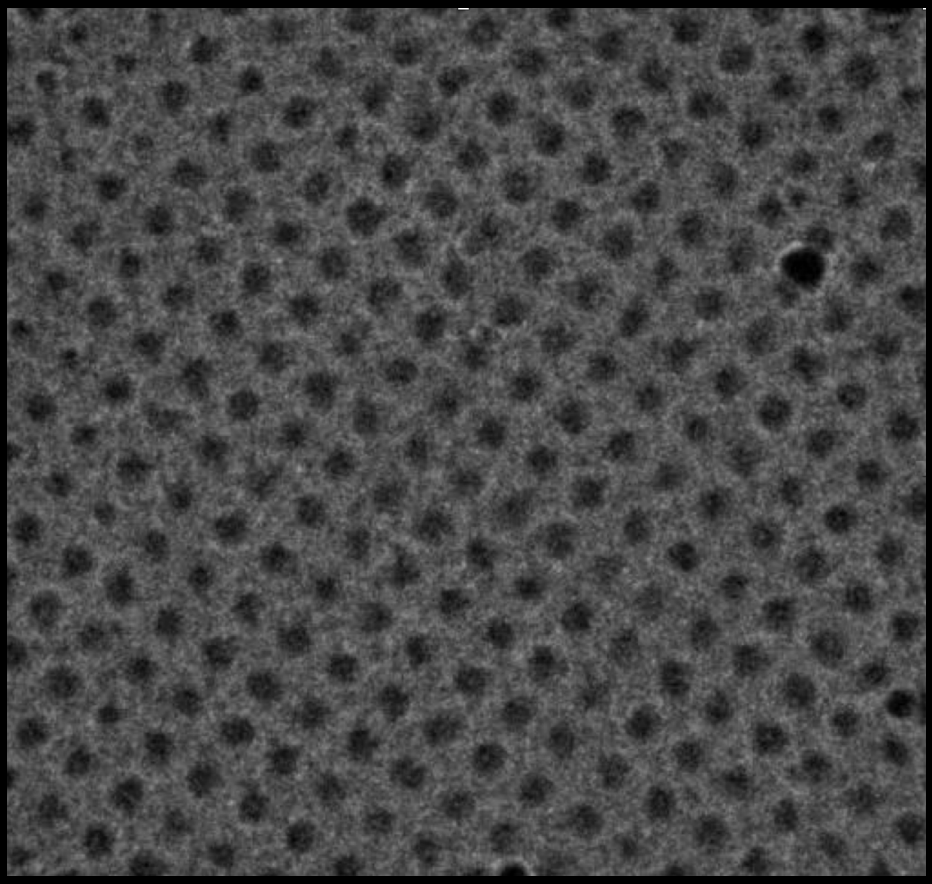

Russo & Henderson (2018a)

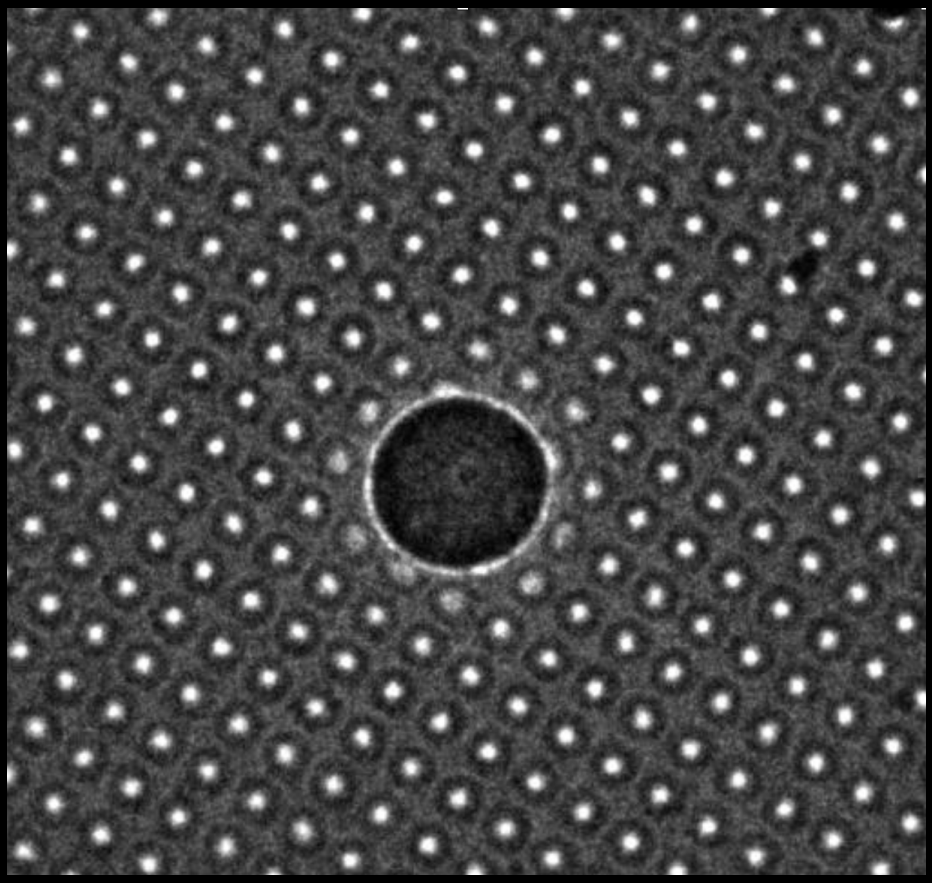

Russo & Henderson (2018a)

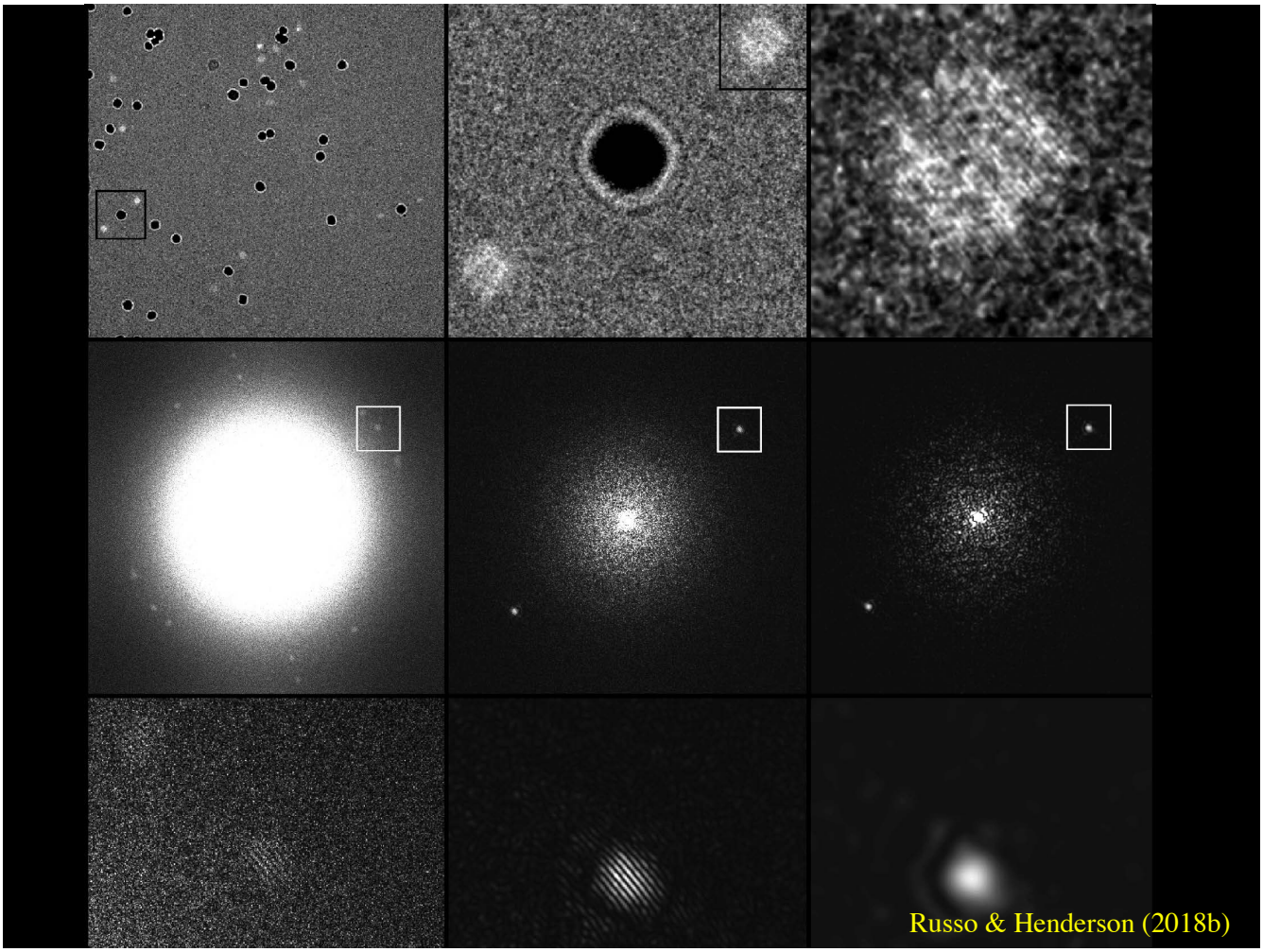
Russo & Henderson (2018b)

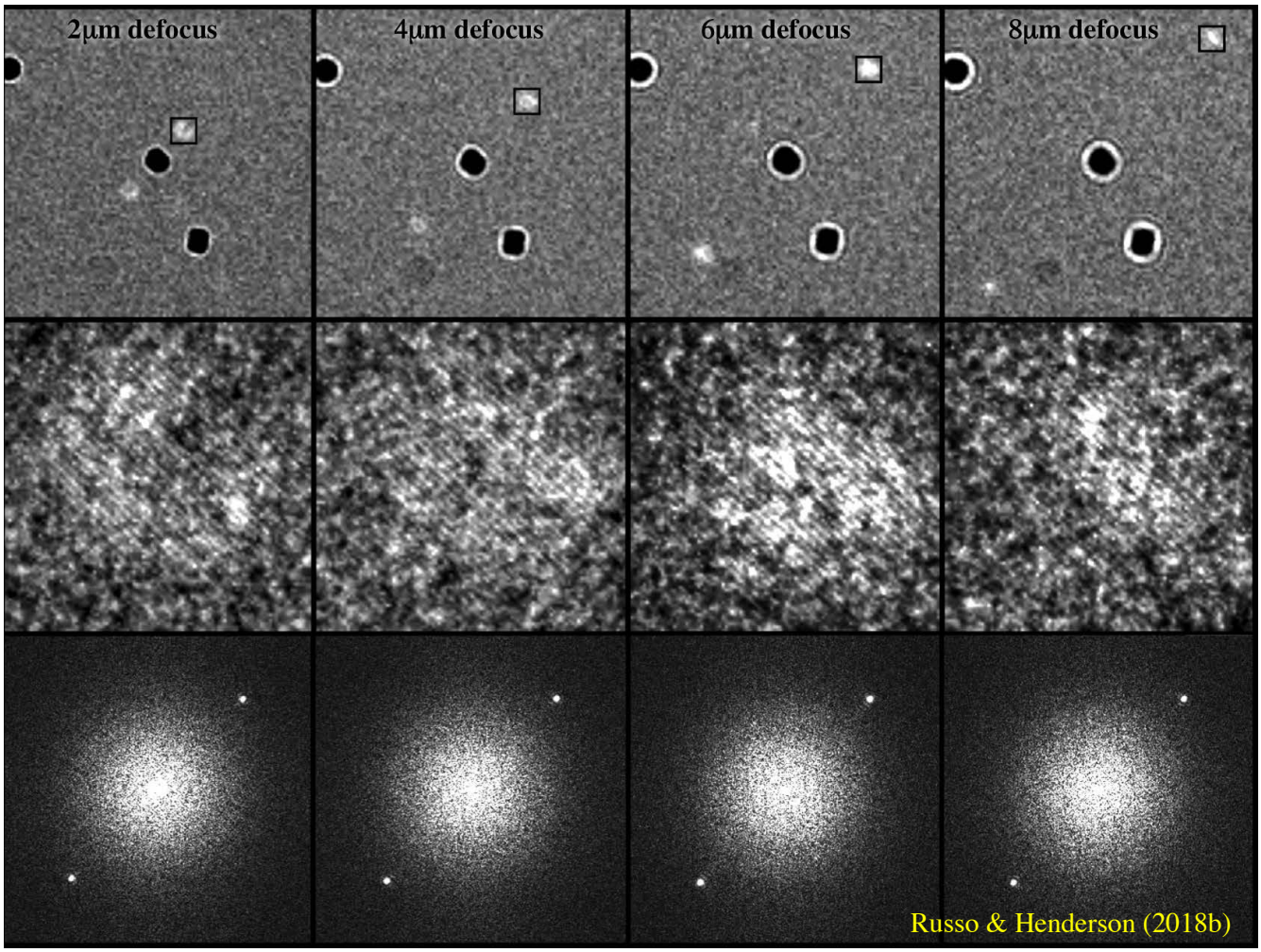
2μm defocus
4μm defocus
6μm defocus
8μm defocus
Russo & Henderson (2018b)

Envelope function for 2.35Å gold nanoparticle fringes – contrast a function of defocus

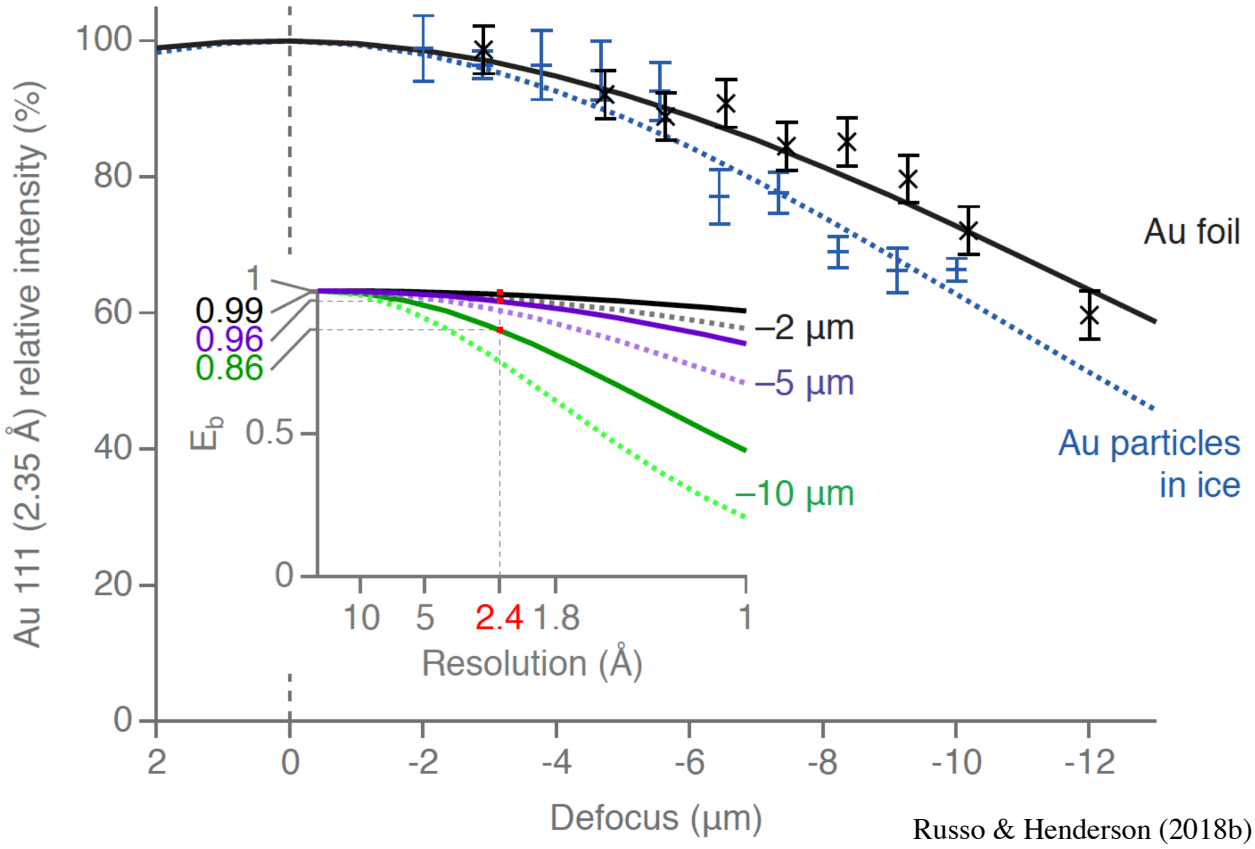

Russo & Henderson (2018b)

[redacted]

Thon rings from ice - McMullan et al, Ultramicroscopy (2015) **158**, 26-32

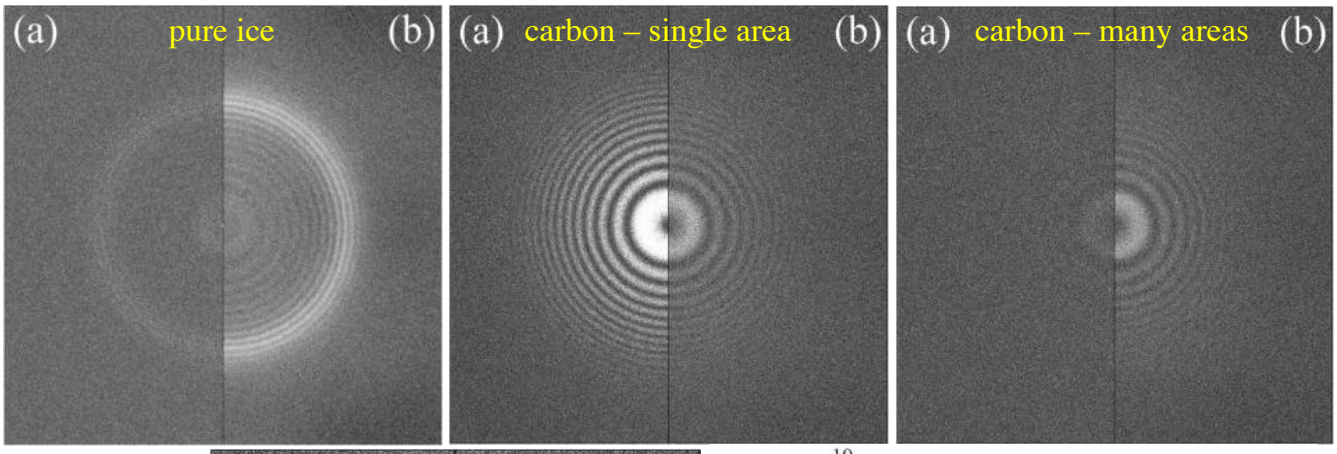

Comparison of ice with carbon under identical conditions

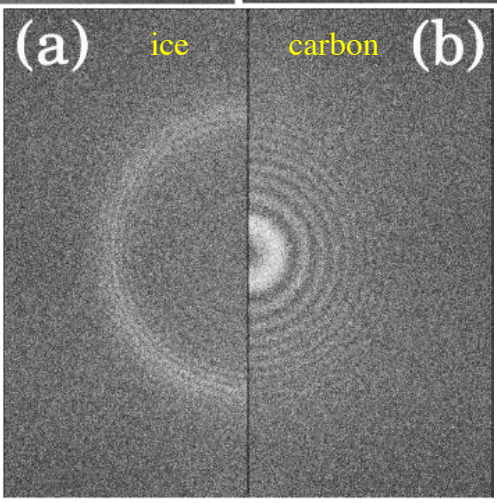

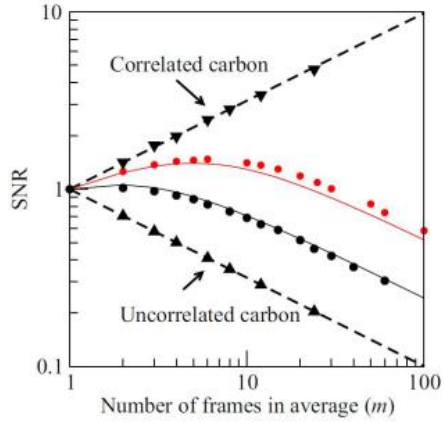

Fig. 6. Relative signal-to-noise ratio of Thon rings in the sum of noise whitened power spectra, $W_{M,m}/W_{M,1}$, from a dose fractionated exposure of M frames as a function of the number of successive images in each power spectrum, m.

Rough Grand Scheme towards a complete physical theory of cryo-EM

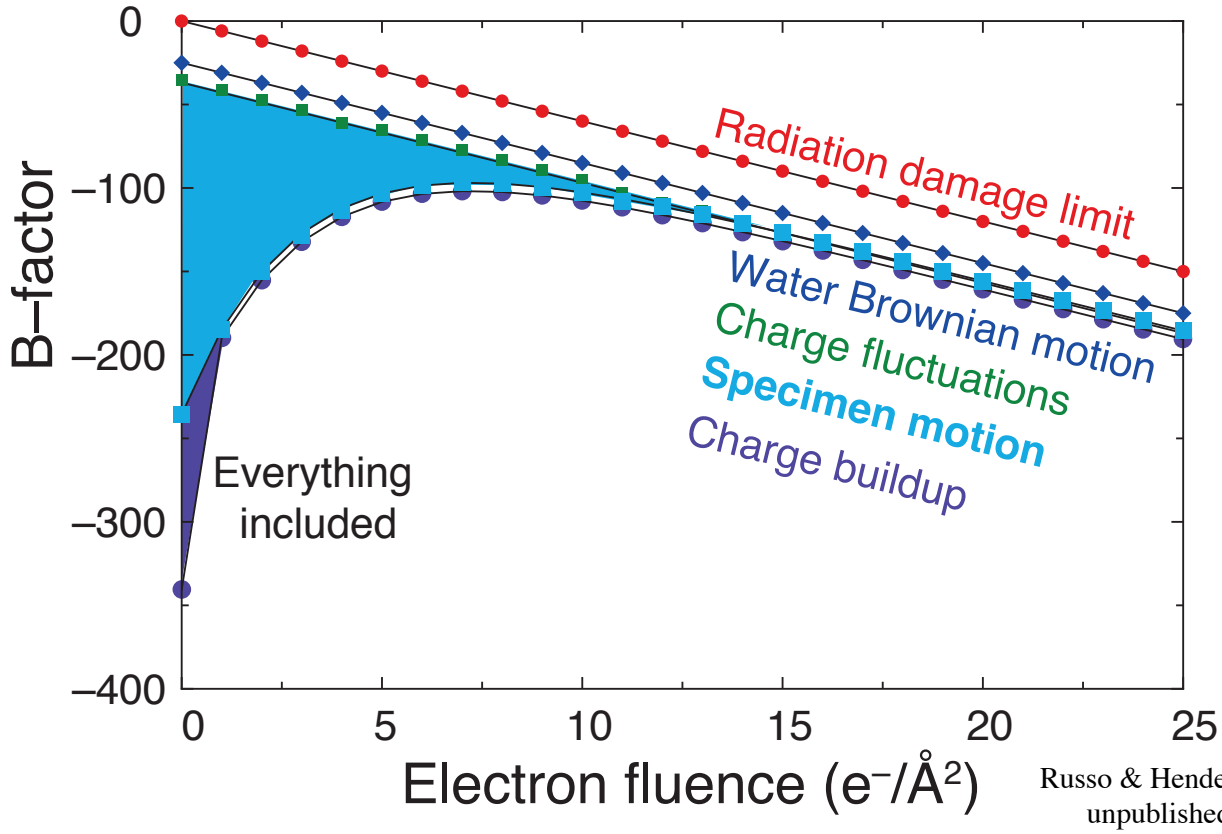

Russo & Henderson unpublished

From Tan et al & Lyumkis, doi: http://dx.doi.org/10.1101/305599; Apr. 21, 2018.

Sub-2Å Ewald Curvature Corrected Single Particle Cryo-EM (AAV2)

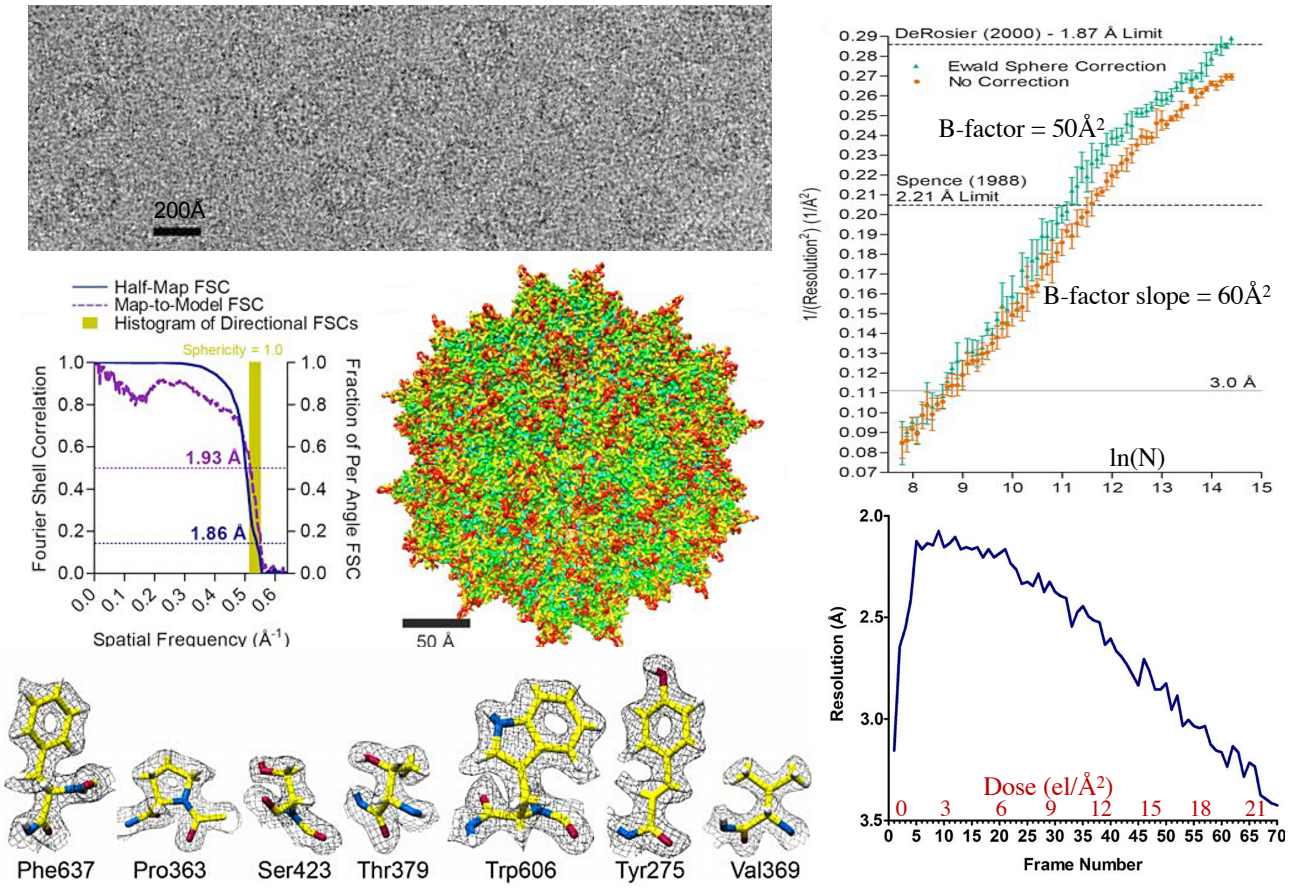

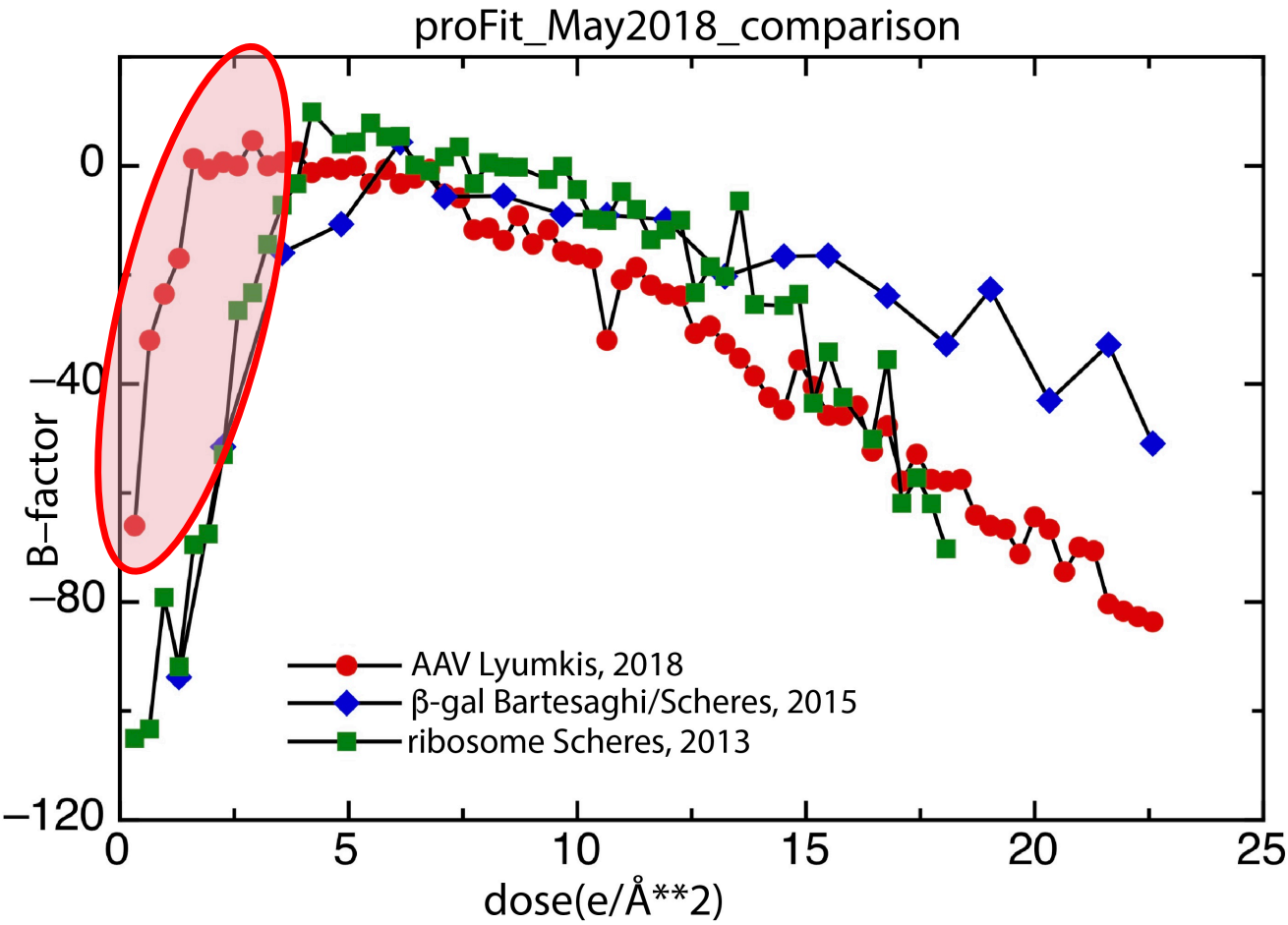

X-ray diffraction of 3D crystals

Temperature-dependent radiation sensitivity and order of 70S ribosome crystals

by Warkentin et al & Thorne (2014)Acta Cryst D70, 2890-2896.

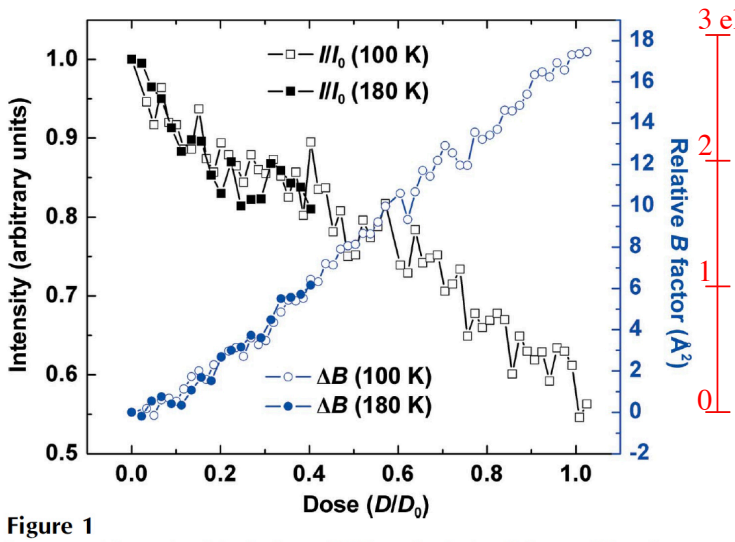

Figure 1
Integrated intensity (black, from *XDS*) and relative *B* factor (blue, from *XSCALE*) *versus* dose at T = 100 and 180 K (samples 1 and 2, respectively) for 70S ribosome crystals. The dose axis has been scaled to D_0 = 50 MGy at 100 K and D_0 = 6.25 MGy at 180 K to facilitate comparison of the dose dependence at these temperatures.

Abstract: All evidence to date indicates that at T = 100 K all protein crystals exhibit comparable sensitivity to X-ray damage when quantified using global metrics such as change in scaling B factor or integrated intensity versus dose. This is consistent with observations in cryo-electron microscopy, and results because nearly all diffusive motions of protein and solvent, including motions induced by radiation damage, are frozen out. *[Have comprehensive theory].*

Gold particle in ice

Image_2017_04_18_23_52_08
Spot01 defocus series all frames
dose = 0.3 el/Å²/frame

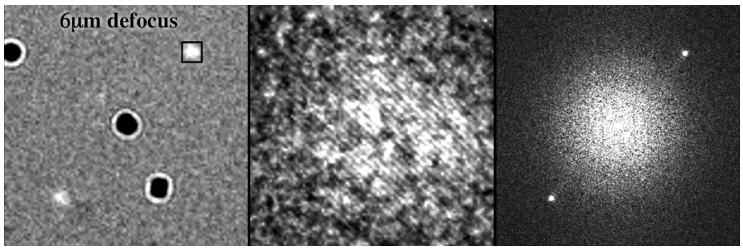

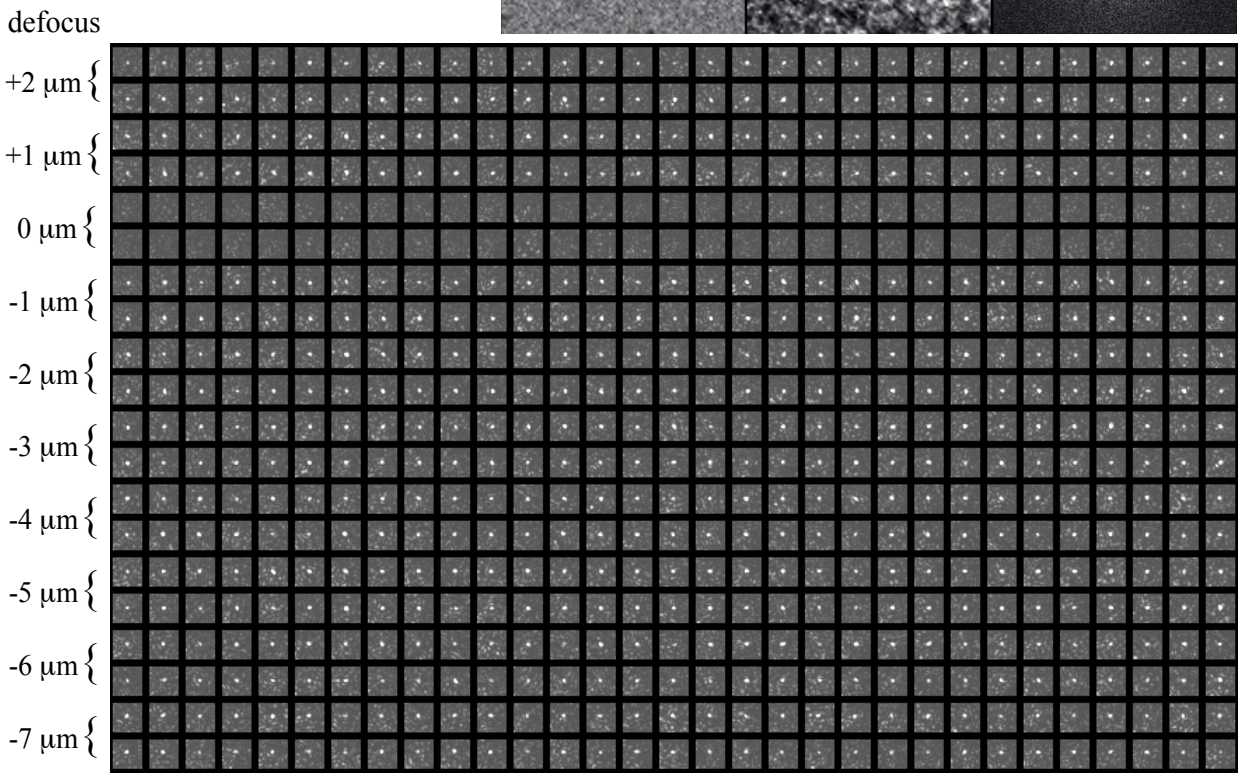

2.2Å resolution β-galactosidase from 100,000 particles with D2 symmetry (400,000 asymmetric units)

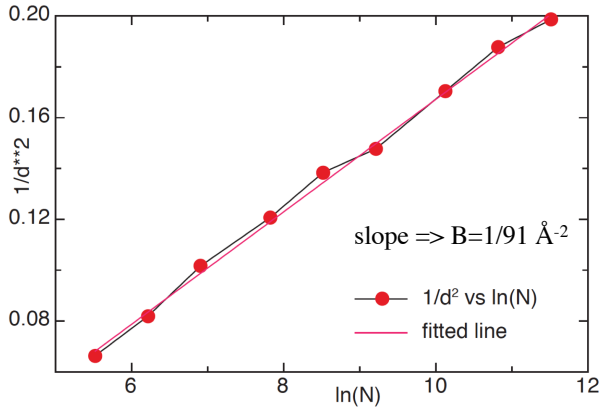

β-galactosidase
data of **Bartesaghi et al & Subramaniam (2015)**
analysis by Sjors Scheres (2017)

slope of plot of $1/d^2$ versus ln(no. ptcles) shows a single reliable B-factor explains the behaviour
For these data, B = 91 Å²
intercept shows 37% mass loss at 45 el/Å²
B-factor plot shows the usual image blurring during first 5-6 el/Å²

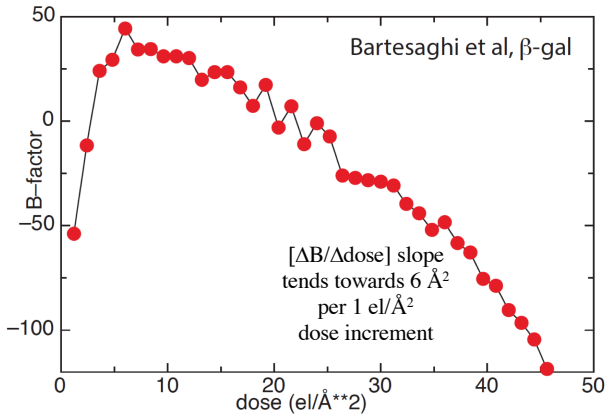

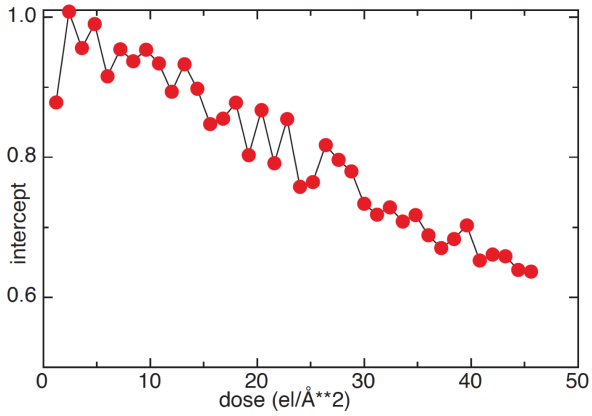

from Relion 3.0: Zivanov, Nakane et al & Scheres, bioRxiv 19 September 2018

Two recent Roseplots with Bfactors of 56 and 66 Å²

β-galactosidase image data from
Bartesaghi et al & Subramaniam (2015)

apoferritin image data from
Wim Hagen

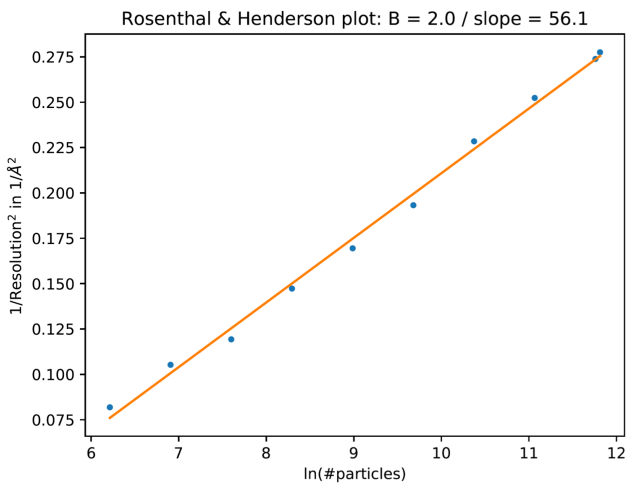

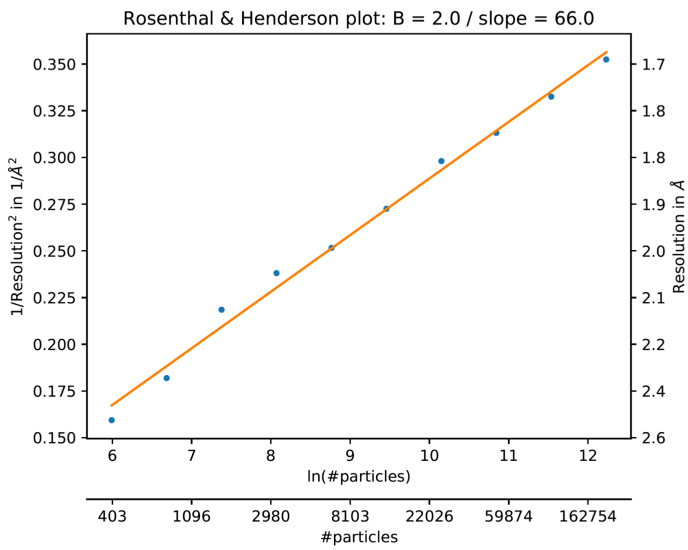

from Relion 3.0: Zivanov, Nakane et al & Scheres, bioRxiv 19 September 2018

Six examples of FSC plots; left panels between two halfmaps; right map-model FSC

influenza haemagglutinin – 40° tilt
apoferritin (Hagen) – beam tilt
P22 virion capsid protein – Ewald

gamma-secretase – auto-process
beta-galactosidase – hi-res
apoferritin (Hagen) – hi-res

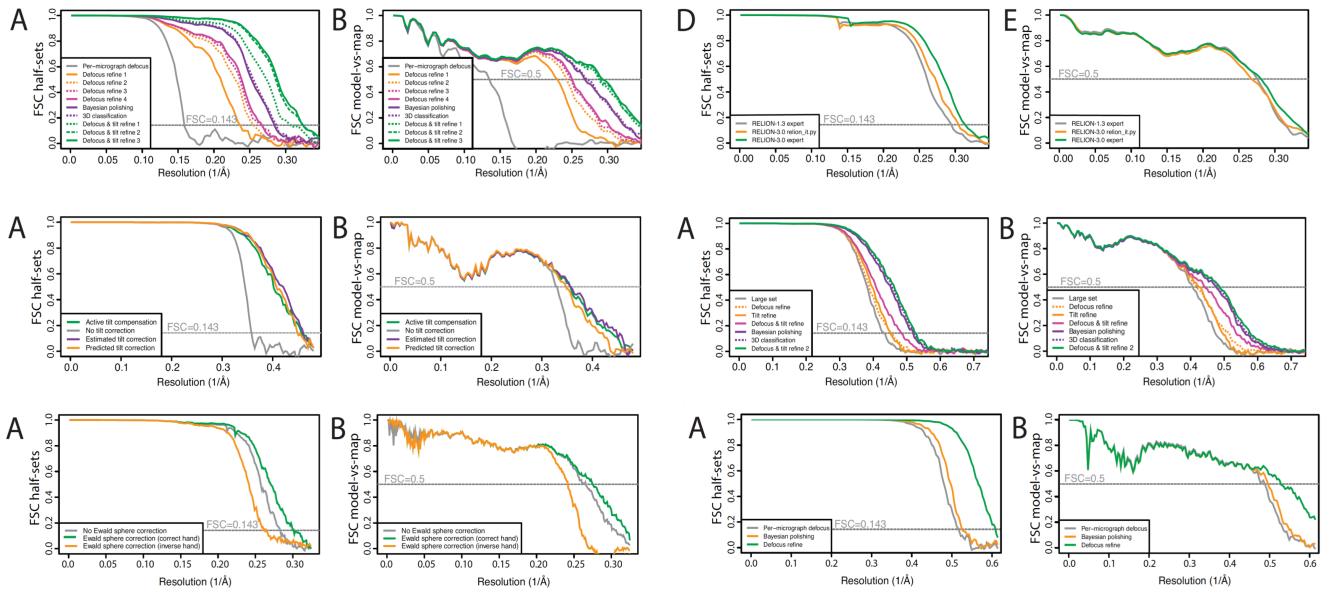

Conclusions

- Radiation damage effects (charging, beam-induced physical motion, mass loss) can be minimised, but damage is unavoidable.
- 10-15 years ago, quality of cryoEM structures was characterised by overall B-factors of 500-1000 Å^2.
- In 2017 the best structures had B-factors of 85-90 Å^2; in 2018 50-60 Å^2.
- Future reductions in overall B-factor to 30Å^2 will give a further drop in number of particles needed; or can use to increase resolution.
- Single particle cryoEM should get better.
- Liquid helium temperature offers the hope of further improvement.

5. Need for affordable cryoEM – from Vinothkumar & Henderson, QRB (2016) **49**, e13 1-25.

The technical details of cryoEM are important and can strongly affect the amount of effort required, the resolution obtained and the ability to resolve multiple states. At present, the performance advantage of 'high-end' cryoEM ('high' because of the large associated capital and running costs of a 300 keV facility) means that those groups and institutions that have access to the best equipment have an enormous advantage over those without such access. Since an installation with equipment that can deliver the best quality images can cost £5 M with annual running cost including management in the range of ~£250 000, this acts as a barrier to providing access for research groups that are not located in a major centre. One solution to the problem would be to provide national or international facilities best illustrated by the success and wide availability of third generation synchrotron sources for X-ray diffraction studies.

The preparation of suitable specimens for cryoEM also requires a lot of preliminary evaluation. Alongside the need for excellent biochemistry, there are many pitfalls along the route to producing a perfect cryoEM grid with a good distribution of single particles that are not denatured at the air–water interface, aggregated, stuck to the support film or suffering from preferential orientations. To overcome this list of typical problems requires (preferably) daily access to a cryoEM facility that is good enough for characterisation of any specimen preparation problems, and for collection of small diagnostic datasets. High electron energy is not necessary in such a diagnostic tool since good images can be obtained at 100 keV. However, the coherence of the electron source makes an enormous difference to the detail visible in the highly defocussed images that are need to observe internal structure in smaller proteins. At present, it is not possible to interpret clearly images of protein assemblies of 150 kDa without the higher defocus that can be used with the much higher coherence of a field emission gun (FEG).

Thus alongside the availability of state-of-the-art 'high-end' electron cryomicroscopes the structural biology field also desperately needs an inexpensive diagnostic cryoEM. Such an instrument is needed for preliminary evaluations, and should be able to achieve good enough resolution (e.g. 4 Å, which is enough to resolve the strands in **β**-sheets and some side-chain information) to evaluate the intrinsic quality of the specimens once a suitable particle distribution has been obtained. This local characterisation of specimens and grids could then feed into and make the best use of regional, national or international resources where higher resolution cryo-microscopes with greater automation could be available. It is certainly unrealistic to expect every laboratory to be able to afford a state-of-the-art facility, which at present needs to include a 300 keV Krios or similar high-end instrument, plus a direct electron detector and possibly also a zero-loss energy filter.

Given the cost of these higher voltage microscopes (due to the need for X-ray shielding and high voltage power supplies), it would be sensible to aim for a 100 or 120 keV instrument for the general market with a FEG electron source (500x brighter than a tungsten filament) and an efficient inexpensive detector at perhaps one tenth of the cost of the 'high-end' instruments.

Peet et al (2019)
Ultramicroscopy

Historical Theory by Bloch/Bethe confirmed in new measurements

Structural information in images for same amount of radiation damage, as a function of electron energy.

Cross section (megabarns)

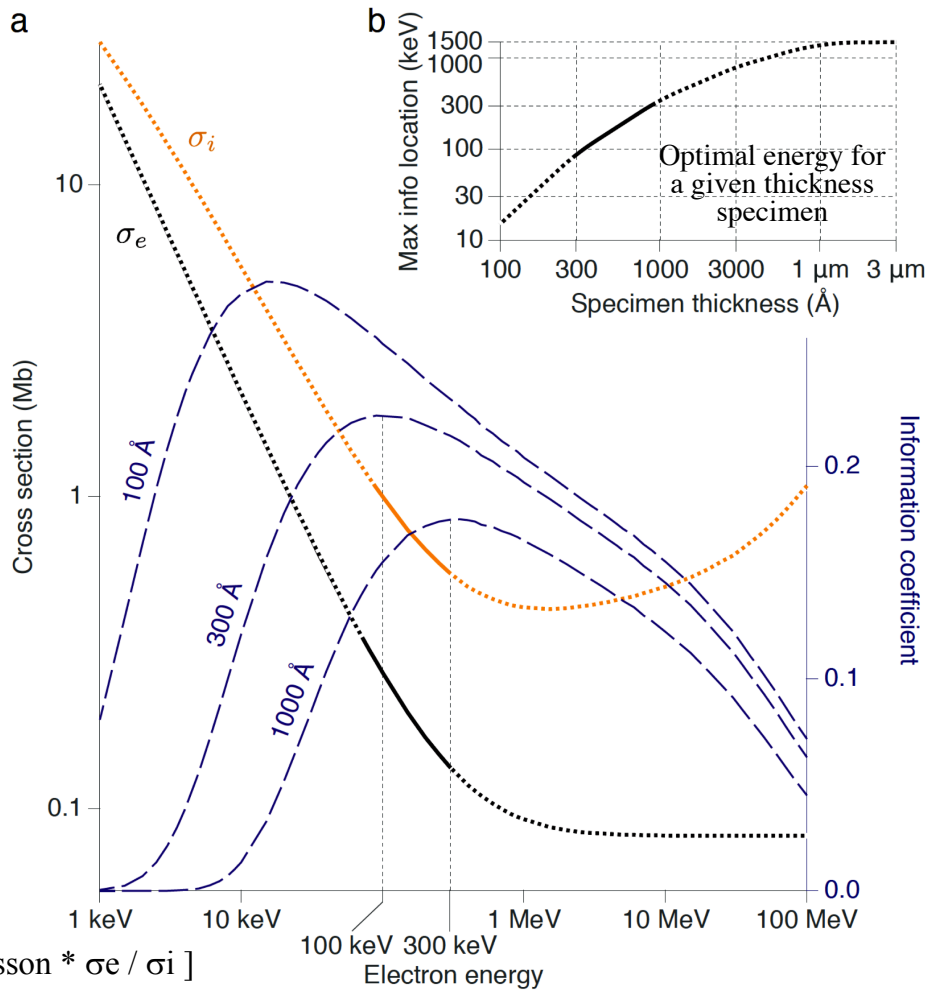

Information ≈ [Transmisson * σe / σi]

Arguments for development of 100 keV cryoEM instrument/tool

- **Inexpensive** - democratizing single particle cryoEM, for hundreds of structural biology groups
- **Theory** - ratio elastic/inelastic cross-section 20-30 % better at 100 keV (c.f. 300 keV)
- **Experiment #1** - measured elastic cross-section follows $\mathbf{c^2/v^2}$ formula exactly
- **Experiment #2** - measured radiation damage el.diff. spot-fading confirms improvement at 100 keV
- **Ewald sphere** - can correct fully for Ewald sphere curvature in computer (implemented in Relion)

Still to be done – publish more papers

- **Radiation damage** - 100/300 keV compare electron diffraction spot-fading on 2D crystals (✔)
- **Proof of principle** - determine some structures using 100 keV/FEG/hybrid-pixel detector (✖)

Obtain full funding for system consisting of :-

- **Configuration** - 100 keV + FEG + at least 2K x 2K CMOS or hybrid big pixel sensor
- **Funding** - commercial or academic or charity ?

When is 300 keV cryoEM better than 100 keV?

- Elastic scattering is 2.0x less; inelastic is 1.5x less at 300 keV, so mean free path is greater and penetration is better. For electron cryotomography or single particle structures bigger than ~600Å, the images will be slightly better.

- The value of ΔE/E will be 3x lower, so the envelope function due to the energy spread of the electron gun and chromatic aberration will be better, giving the potential for resolutions beyond ~3Å (e.g. apoferritin at 1.5Å, β-galactosidase or AAV at 1.8Å).

Micrograph of apoferritin at 100 keV with 3 Å pixels

Dectris Eiger X 500K hybrid pixel detector

before and

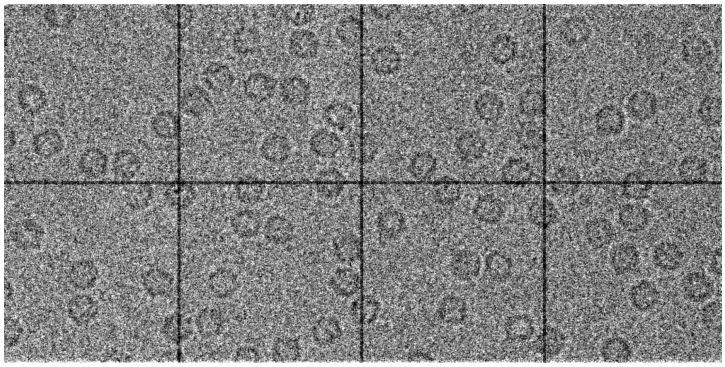

Before has 8 tiles of 256 x 256 pixels with gaps

after bright-field correction

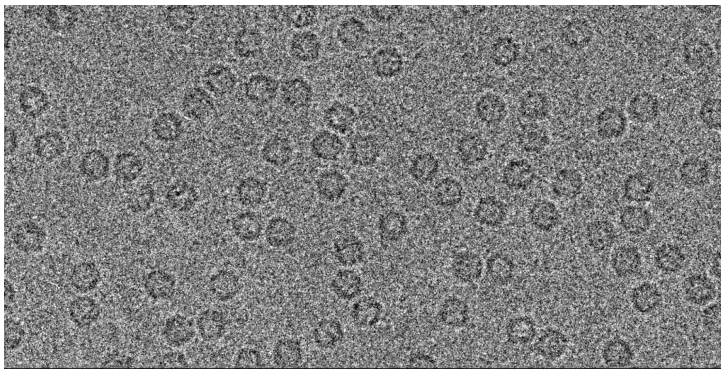

After shows 1030 x 514 pixel image; two pixel gap is interpolated

Greg McMullan, Sept 2018

CryoEM at 100 keV: a demonstration and prospects

MRC Laboratory of Molecular Biology, Cambridge CB2 0QH, UK
K. Naydenova, G. McMullan, M.J. Peet, Y. Lee, P.C. Edwards, S. Chen, E. Leahy, S. Scotcher, R. Henderson and C.J. Russo *

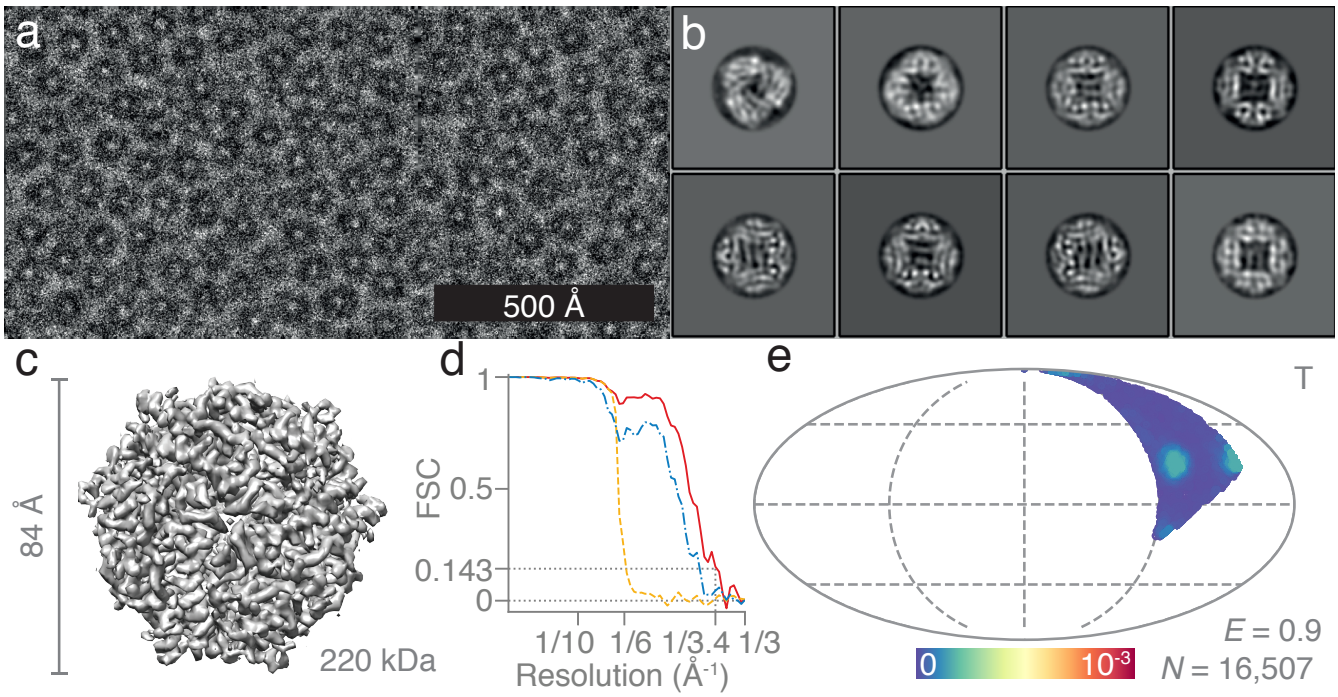

Figure 5